CHEMISTRY
A EUROPEAN JOURNAL

Tuning Helical Chirality in Polycyclic Ladder Systems

*Michel Rickhaus, Oliver T. Unke, Rajesh Mannancherry, Linda M. Bannwart, Markus Neuburger, Daniel Häussinger, and Marcel Mayor**

[*] M. Rickhaus, O. T. Unke, R. Mannancherry, L. M. Bannwart, Dr. M. Neuburger, Dr. D. Häussinger, Prof. Dr. M. Mayor
Department of Chemistry
University of Basel
St. Johanns-Ring 19
4056 Basel, Switzerland
E-mail: marcel.mayor@unibas.ch

Prof. Dr. M. Mayor
Institute for Nanotechnology (INT)
Karlsruhe Institute of Technology (KIT)
P. O. Box 3640
76021 Karlsruhe, Germany
Lehn Institute of Functional Materials (LIFM)
Sun Yat-Sen University
Guangzhou, China

[**] The authors acknowledge financial support by the Swiss National Science Foundation (SNF).

Abstract:

Conceptually and experimentally, a new set of helical model compounds is presented herein that allow to investigate correlations between structural features and their expression in the secondary structure. As model system serves a cross-linked oligomer with two strands of mismatching lengths that are connected in a ladder-type fashion. Compensation of the dimensional mismatch leads to the adoption of a helical arrangement. A strategically placed relay ensures the continuity and uniformity of the helix. Upon exchanging of the heteroatomic linkage, the helix responds by increasing or decreasing the torsion of the backbone. Inversion of the relay's substitution pattern causes a distortion of the structure, while maintaining the directionality of the helix. Based on a short synthetic protocol with a modular precursor, four closely related "*Geländer*" oligomers ("Geländer" is the German word for bannister) were accessed and fully characterized. X-ray diffraction analysis for one representative of each helical arrangement and complementary computational studies for the remaining derivatives allowed studying the impact of the alterations on the secondary structures. Isolation of pure enantiomers of all the new "*Geländer*"-oligomers provided insight into the racemization kinetics and the racemization barrier. *In silico* simulation of the electronic circular dichroism spectra of the model compounds enabled to assign the helicity to the isolated samples.

Introduction

Circular staircases, propellers and screws are fundamental examples of helical structures that have fascinated designers, architects and researchers alike. The formation of these chiral structures on a microscopic scale has been key to relate chirality to structure and structure to function.[1–10] Among the most prominent examples for such stereocenter-free, chiral molecules are the polyaromatic helicenes. Exclusively due to steric interactions, the annulated rings adopt a spring-like configuration that resemble the steps of a helical staircase. Their exceptional optical properties, their stability and versatility in combination with their structural beauty and simplicity, have made them into important model systems for both chemists and physicists. An excellent representation of these fascinating structures can be found in the recent reviews celebrating 100 years of helicenes.[11-13]

Fritz Vögtle and coworkers designed and investigated a fundamentally different polyaromatic system 17 years ago which he labeled "Geländer"-molecules (Geländer is the German word for bannister).[14,15] While helicenes and their related structures consist of rings which are arranged perpendicular to the

propagation axis of the helix, “Geländer”-oligomers are axially chiral – here the orientation of the rings is along the propagation axis. The fundamental characteristics are already present in bridged biphenyls: An alkyl linker bridges the phenyl rings, locking them in a specific conformation (*M* or *P*).[16-22] Adding a third ring (also conformationally locked by an alkyl bridge) results in Vögtle's terphenylic “Geländer”-oligomers. The obtained structures show very similar chiroptical properties and conformational stability to the shorter helicenes. However, due to the molecules symmetry both biphenyl-junctions are equivalent and can adopt either a *M* or *P* conformation, resulting in three possible stereoisomers: *MM* and *PP* which are enantiomeric and the achiral *meso* compound (*MP*/*PM*). If the formation of the bridges is unspecific and independent of the other, the resulting distribution of conformers is statistical (*MM* and *PP* each 25 %, *meso* 50 %). And indeed, in the classical bannister oligomers, 50 % of the adopted conformers are achiral, making these systems less suited as model compounds for extensive chiroptical studies – especially as their interconversion is dynamic, resulting in degrading of chiroptically pure samples. To date, these delicate studies require storage and investigations of the samples at sufficiently low temperatures and within narrow time windows.

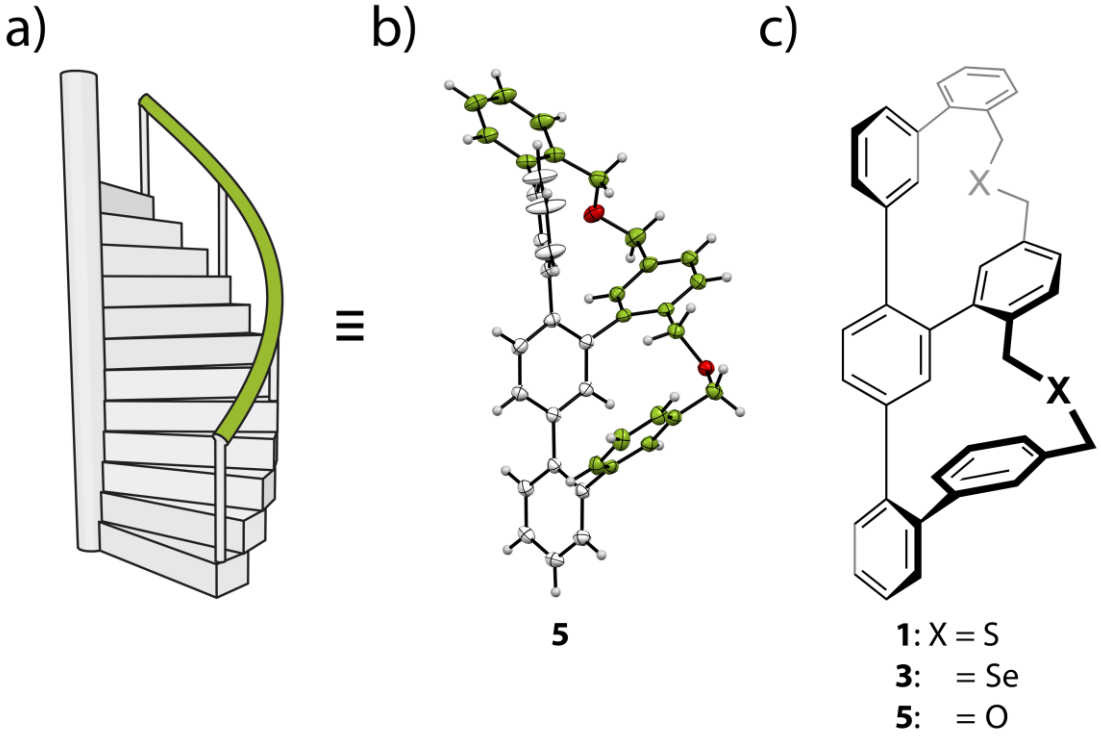

Figure 1: Overview of bannister-oligomers. a) Helical staircase with continuous bannister (green). b) Single crystal structure of the helical oligomer **5**, which exhibits a continuous, bannister-like arrangement. c) Schematic representation of the bannister oligomers **1**, **3** and **5** containing various heteroatoms.

We have recently addressed this issue by developing a related, ladder-like system,[23] which can exclusively adopt either an *M* or *P* conformation (*Figure 2*). With Vögtle's systems in mind, the terphenylic backbone is connected to a longer oligomer with individual linkages to each ring of the backbone. The extended oligomer then induces helicity due to spatial constraints. The sense of twist induced by one part of the bridge is communicated across the entire structure with the midsection of the longer oligomer acting as a relay. Accessing the desired structure required a time-consuming development of the synthetic strategy and was finally obtained in 12 steps.[23,24] The purification steps of the target structure were particularly demanding, resulting in significant deviations in the isolated yield. To our surprise, the isolated yield did not exceed 28 % and the fate of the remaining starting material remained ambiguous. The obtained purified structure showed high temperature, air and moisture stability once isolated. Detailed investigations by 1D and 2D NMR, Electronic Circular Dichroism (ECD) spectroscopy and X-Ray diffraction analysis demonstrated the viability of the concept. Two enantiomeric helices were found with a very well defined stereodynamic behavior, which allowed not only to follow the racemization by CD spectroscopy but also to determine the racemization barrier to be 97.6 kJ/mol at 25 °C.

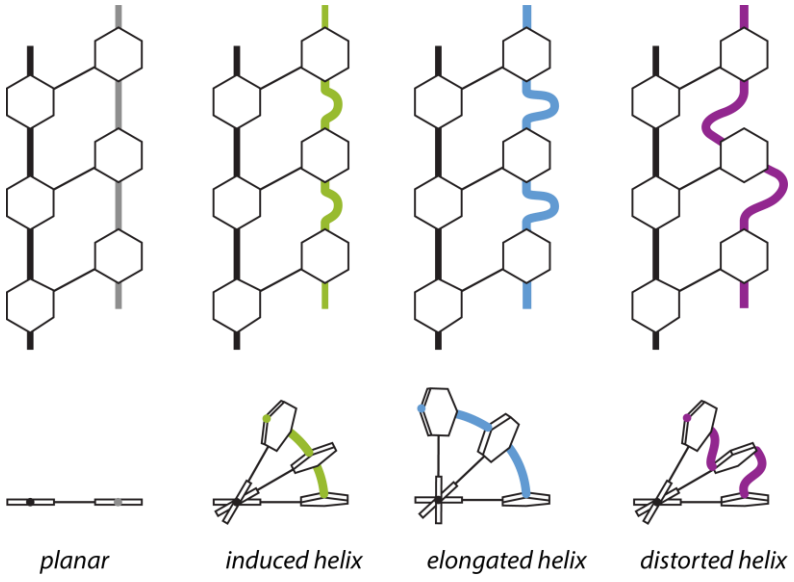

Figure 2: Conceptual representation of a helical ladder structure (*left*) and the concepts for induction, elongation and distortion of the original helix (*middle and right*). Induction of helical chirality is achieved by elongation of the segments on one side of the ladder while keeping the length on the other (green). Rotation of the longer segment around the shorter leads to a helical arrangement. Elongation of the helix is obtained by increasing the length of both longer segments (*blue*) while inversion of the substitution pattern of the relay leads to discriminated ring sizes (purple) resulting in distortion of the helix.

Motivated by these preliminary results, we wondered to what extent the chemical nature of the bridge determines the molecule's physical properties like the structural stability of the helix. From a synthetic point of view, we were still curious concerning the fate of the remaining material in the final cyclization step. The new focus was set towards chemically altering the bridging structure in order to investigate its effect on chemical features like integrity and stability, but also on physical-chemical properties like the extent of structural twist in the helix and its influence on the racemization barrier. To answer these, and related questions, we devised several strategies to overcome the limitations of the initial diether structure. Ideally suited to precisely alter the extent of twist in the helix is the linking heteroatom in the bridging structure and we became thus interested in exchanging the oxygen for the larger sulfur or selenium. Consequently, we aimed for a modular approach, incorporating the heteroatom at a late stage of the synthesis.

Herein we like to present our new versatile synthetic approach to various polycyclic ladder systems and the study of their properties and stereodynamics. The assembly of a nonspecific tetrabrominated precursor allowed to efficiently introduce other chalcogens as heteroatoms at the last stage of the synthesis. Exchanging oxygen for the significantly larger and softer sulfur and selenium allowed fine-tuning of the helical structures (*Figure 2*, *blue*). In addition, the variation in the connection of the middle ring gave access to distorted helical structures with different twists in both junctions (*purple*). The impact of these variations on the structure, especially on the degrees of twist and the racemization dynamics are studied and reported in detail.

Results and Discussion

Synthesis of precursor 11

The projected incorporation of a range of heteroatoms required a modular approach. A common denominator of the heteroatoms sulfur and selenium is their occurrence as simple sodium salts (Na_2S and Na_2Se). Contrary to the corresponding sodium oxide, these salts are relatively stable and safe to handle while showing excellent nucleophilicity. In the context of possible synthetic pathways, the employment of these salts as source of the heteroatom allows to share the same precursor (**11** in Scheme 1). After incorporation of the chalogen by a nucleophilic displacement of a suitable leaving group, the heteroatom remains nucleophilic enough to initiate the desired subsequent macrocyclization without an intermediary

workup. Besides, using a versatile leaving group allows the incorporation of other promising linkages (e.g. amines or metals).

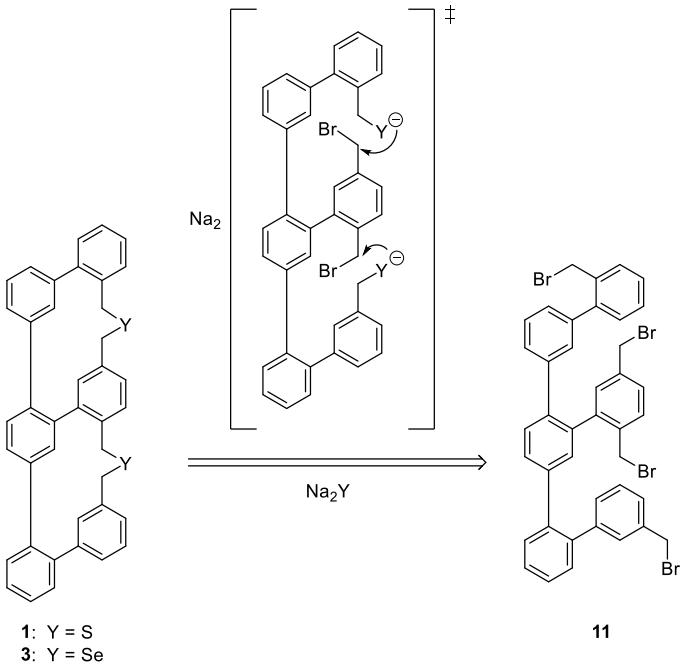

Scheme 1: Modular strategy based on a tetrabromo precursor (**11**) to incorporate the desired heteroatom and subsequently initiate macrocyclization *in situ*.

In principle the required terabromo precursor is accessible by expanding on the strategy previously described.[24] However, precursor **11** showed potential for the development of more efficient methodologies. A careful disconnection of the target structure revealed that in any case at least three borylations are necessary to keep the overall amount of required orthogonal functionalities minimal. Borylations are often challenging and can result in fragile intermediates, especially with sterically more evolved structures. A possible starting point would be the symmetric, commercially available, diborylated benzene **6** (Scheme 2) that features two of the three boronic moieties. Statistically attaching fragment **A** then gives the mono coupled intermediate **7** featuring the third boronic moiety for a subsequent cross-coupling of the next fragment (**B** in that case). At that stage we became interested whether we could use the boronic ester as a directing group to introduce the next handle at the *ortho* position. According to literature, boronic esters are generally only weakly directing functionalities. Wang and coworkers[25,26] impressively demonstrated that under mild Lewis acidic conditions regioselective halogenations of borylated aromatic systems is possible - and that any other substituents (even methyls) will define the location of the halogen. System **7** features three rings suitable for halogenation. However, we reasoned that under the described conditions the boronic moiety will define the chemoselectivity in the

halogenation step, while the adjacent phenyl ring will determine its exact position (*para* over *ortho*). Introducing a bromine would still allow to subsequently cross-couple first the boronic moiety with fragment **B** bearing the more reactive iodine leading to intermediate **9** which is the first fragment *en route* as previously described. We can then follow the route to intermediate **10** using the remaining bromine as a handle to attach fragment **C** before converting **10** into the precursor **11**. Indeed, we found that the statistical cross-coupling of **6** with **A** gave the desired mono coupled intermediate **7** along with the twofold coupled derivative (60:40 by GC-MS). While the conversion was excellent for a statistical reaction the purification was usually accompanied by loss in yield due to the metastability of **7** towards column chromatography. The subsequent bromination proceeded in conversions typically round 75 % (isolated yield: 49%) at the predicted position as determined by GC-MS. Only minor amounts of the second *ortho* derivative was observed and overbromination was efficiently prevented by slow addition of solid NBS. Due to the tendency of **8** to undergo deborylation – even more than **7**, possibly resulting from the increased steric strain – the subsequent attachment of commercially available **B** was best carried out without extensive purification. Pleasingly, the cross-coupling underwent a complete transition to **9**. Our own, previously published methodology[24] gave access to **10** which was efficiently transformed to **11** by *Appel*-type bromination (61 %).

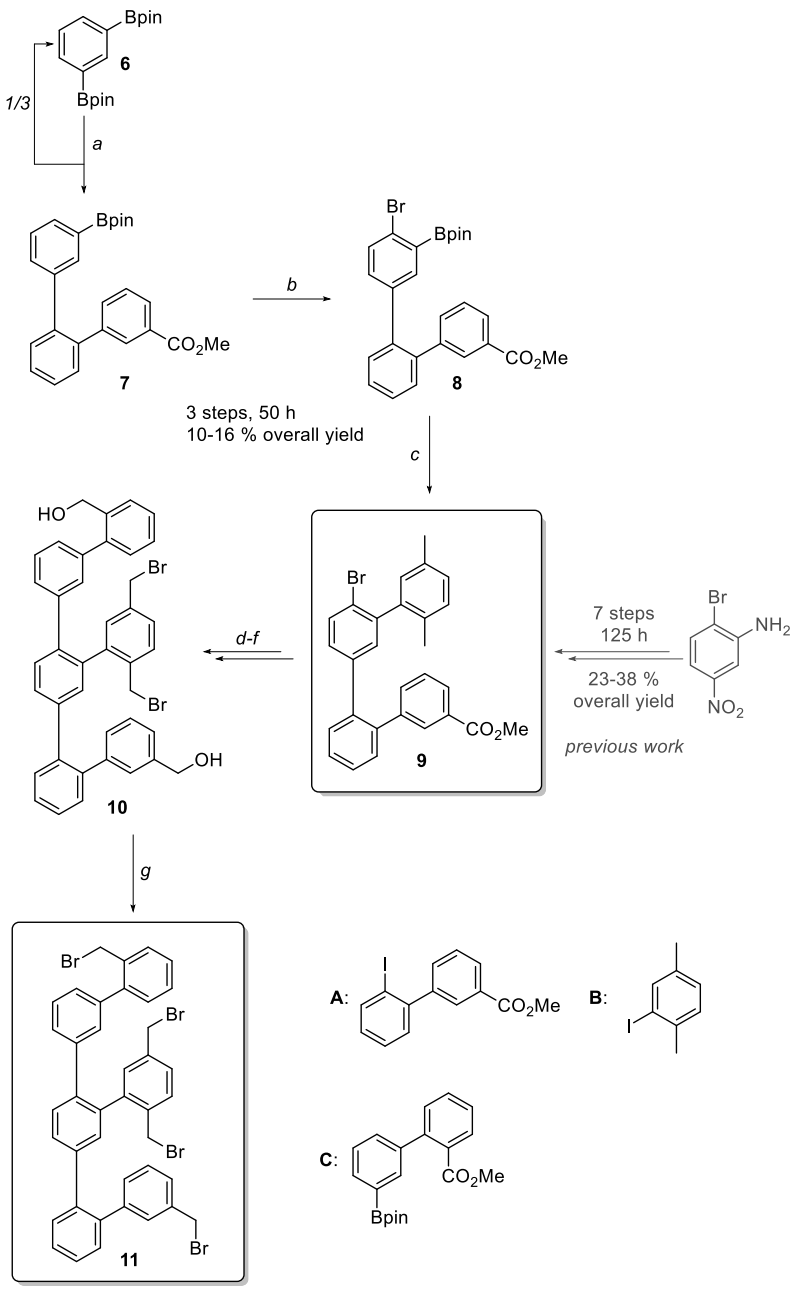

Scheme 2: Synthesis of target precursor **11**. Reaction conditions: a) **A**, $Pd(PPh_3)_2Cl_2$, K_2CO_3, 1,4-dioxane/MeOH 10:1, 60 °C, 2 h, 32 %; b) NBS, $AuCl_3$, DCE, 60 °C, 15 h, 31-49 %; c) **B**, $Pd(PPh_3)_2Cl_2$, 1,4-dioxane/MeOH 4:1, 60 °C, 15 h, >99 %; d) **C**, SPhos Pd G2, K_2CO_3, toluene/H_2O 4:1, reflux, 1-3 d, 50 %; e) NBS, DBP, CCl_4, 75 °C, 1 h, 87 % to >99 %; f) DIBAL-H, DCM, room temperature, 30 min, >99 %; g) PBr_3, DCM, room temperature, 1 h, 61 %; Bpin=4,4,5,5,-tetramethyl-1,3,2-dioxaborolane, DBP=dibenzoylperoxide, NBS=N-bromosuccimide, DCE=dichloroethane.

Synthesis and characterization of the oligomers 1-4

With **11** in hand we first turned to the sulfur derivative **1**. Much to our delight the macrocyclization was both fast and selective. The direct transformation into the twofold cyclized target structure allowed for the first time to observe the formation of the constitutional isomer **2** as direct consequence of the rotational equilibrium in **11** (Scheme 3). Due to the high similarities of the structures a conventional separation of **1** and **2** was not possible giving a 1:1 mixture in very satisfying yield (76 %; diether **5**: 28 %). In the oxygen derivative **5**[23] the heteroatom was present as a hydroxy group which required deprotonation by a strong base (NaH) before cyclization occurred. We found that the second cyclization would only proceed to a satisfying extend if the structure was purified after the first cyclization. However, only one of the four possible mono-cyclized intermediates was stable enough to be isolated resulting in the observed deviations in yield and prevented to isolate the constitutional isomer. In the case presented here for **1** and **2** the heteroatoms initiate the macrocyclization without the need of an external base directly after incorporation. The isolation of any intermediate becomes obsolete and results in the improved yield of both isomers. From the distribution of the constitutional isomers we conclude that the relay undergoes fast rotation round the central aryl-aryl bond.

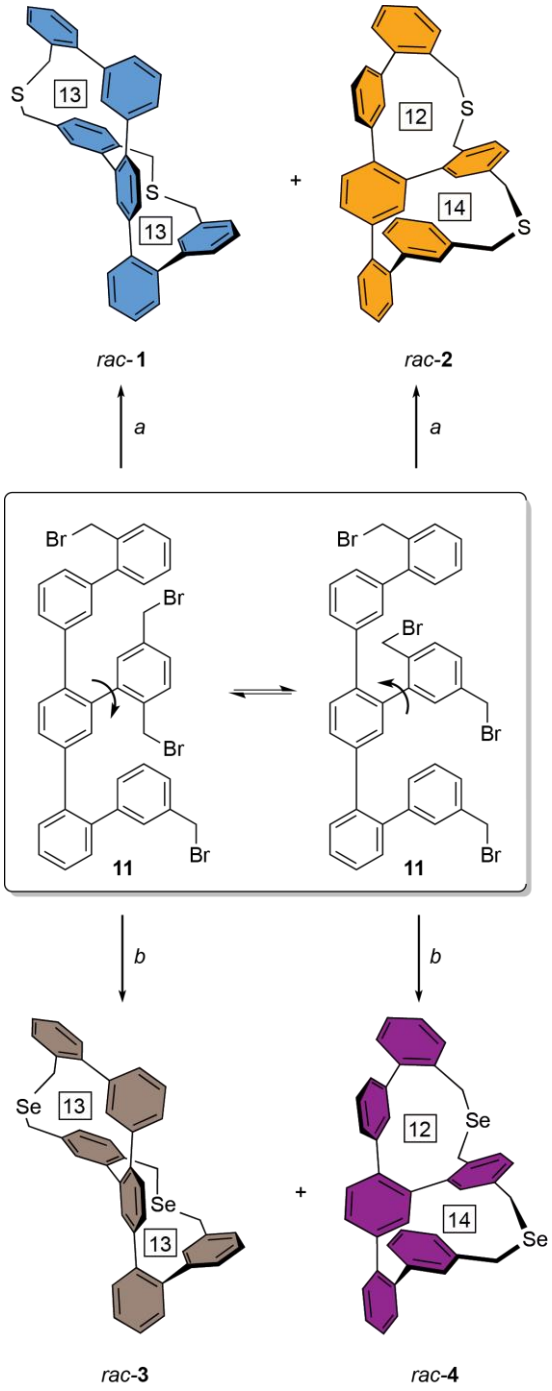

Scheme 3: Synthesis of target compounds **1** - **4**. Reaction conditions: a) Na_2S, EtOH/toluene 1:1, room temperature, 4.5 h, 76 % as 4 isomers; b) Na_2Se, EtOH/toluene 3:2, room temperature, 2.5 h, 50 % as 4 isomers. The numbers in the square boxes correspond to the number of atoms in each macrocycle.

While conventional purifications were unsuitable, the isolation of the four isomers (2 pairs of enantiomers) was possible by chiral HPLC (Chiralpak IA, 2 mL/min, 99:1 hexane/*i*PrOH, 18 °C, Figure 3, a-d) separation directly after a preliminary workup to remove the ionic byproducts. Indeed, all four isomers were observed, while two of them (**1b**/**2b**) did not show baseline separation and required subsequent chromatography (chiral HPLC). Conveniently, the addition of 1 % of DCM allowed to reasonably resolve the mixed peak. The protocol was reliable enough that upscaling to a semi- preparative column was possible, which allowed to obtain all isomers in amounts suitable for subsequent unambiguous characterization by 1D- and 2D-NMR spectroscopy and High Resolution ESI Mass Spectrometry (HR-ESI-MS). As expected for constitutional isomers, all obtained masses were identical but required addition of a sodium source to be detected by ESI-MS. The well ordered, helical oligomer pair **1a,b** showed NMR spectra that were similar to those obtained for the oxygen derivative **5**, and were suitable for full assignment by 2D-NMR spectroscopy. The mismatched helix **2**, on the contrary, gave broad signals especially for the benzylic hydrogens (see SI S25) and to lesser degrees also for the aromatic hydrogens of the bridge, pointing towards the presence (and interconversion into) more than one species with related chirality. It is important to note, that a broadening of NMR signals points at fast structural changes on the NMR timescale and is very likely not an indicator of an accelerated racemization process. We suspect that the deformed helix profits from higher degrees of freedom and can adopt multiple conformations of the bridge with similar overall energies. The sharp signals of the aromatic protons of the backbone indicate that interconversion of the helices is present on a timescale much larger than the one observed by ^{1}H-NMR which was confirmed by kinetic studies at a later stage. By incrementing the temperature, adoption of all the different conformations should be facilitated resulting in an averaged structure. Indeed, variable temperature (VT) NMR spectroscopy of *rac*-**2** in *d2*-tetrachloroethane (TCE) at 105 °C (see SI S25) revealed a well resolved spectrum with sharp, well defined peaks. This eventually allowed to record 2D-NMR spectra and fully assign all observed peaks and confirming the predicted constitution of **2**. Furthermore, we observed for one aromatic hydrogen of **2** a pronounced high-field shift (5.61 ppm at 378 K). Most likely this proton is facing an aromatic ring directly in a reasonably rigid arrangement and is subjected to a high ring current. This signal is comparably well resolved above room temperature with a stable shift – further supporting a slow racemization process on the NMR timescale, which would move that hydrogen out of the ring current during the transition of one enantiomer to the other. Once purified, both **1** and **2** were found to be stable towards air and moisture and even reasonably towards silica.

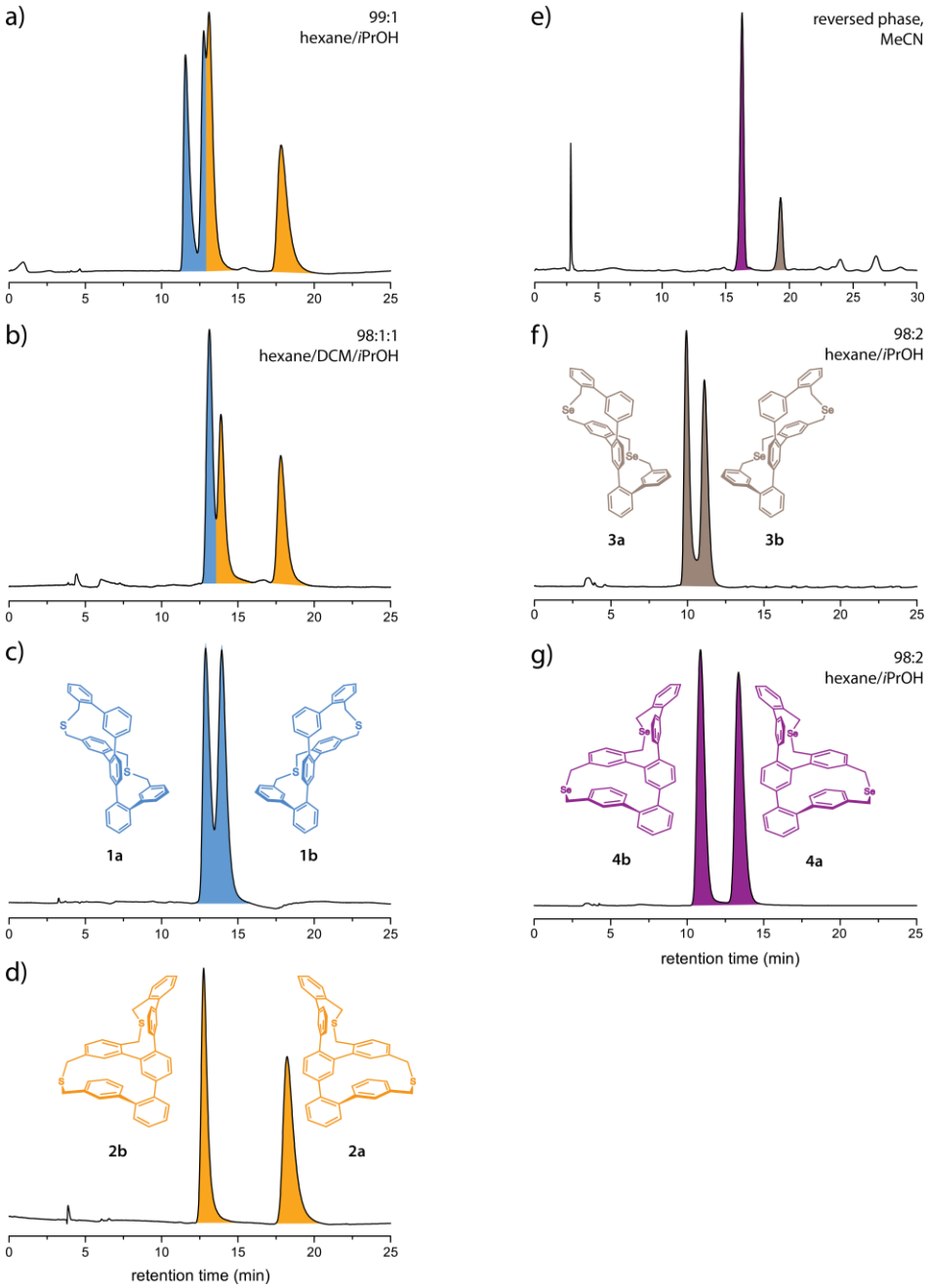

Figure 3: Traces of the chiral HPLC separations (Chiralpak IA, 18 - 19 °C, 1 - 2 mL/min). a) Separation of **1** and **2** in a mixture of 99:1 hexanes and *i*PrOH. All four isomers (**1a,b** in blue and **2a,b** in orange) can be observed. The middle peak is a mixture of **1b** and **2a**; b) the addition of 1 % DCM allowed to separate **1b** from **2a**; c) resolution of **1a** and **1b**; d) resolution of **2a** and **2b**; e) reversed phase separation (Reprosil C18, MeCN, 1mL/min) of the obtained reaction mixture of **3** (brown)and **4** (purple); f) chiral resolution of **3a** and **3b** (98:2 hexanes and *i*PrOH); g) resolution of **4a** and **4b**.

Encouraged by the transition of **11** into the sulfur targets **1** and **2** we aimed at accessing the selenium bridged derivative **3** (and potentially **4**) which we expected to show diminished stabilities to the well documented ease of oxidation and thermal liability of the selenium atoms. For the cyclization of the sulfur oligomers, we used the highly nucleophilic Na_2S as sulfur source, which is comparably stable and can be used without excessive precautions. However, the corresponding selenium salt Na_2Se is much more reactive (both towards the desired nucleophilic substitutions as well as oxygen and water) and toxic and has to be handled in a glove box. Drop-wise addition of Na_2Se in EtOH/toluene (4:1) to a diluted solution of the precursor **11** in EtOH/toluene (1:1) at RT over 2 h resulted in full consumption of the starting material. Due to the instability of the formed products towards conventional chromatography, the reaction was monitored by DART-MS and reversed phase HPLC (Reprosil C18, MeCN, 1 mL/min). By HR-ESI-MS the two most intense peaks were attributed to the desired oligomers **3** and **4**. To our surprise and in contrast to the sulfur derivatives, the desired oligomers did no longer form in a 1:1 ratio – one of the constitutional isomers was preferably formed (about 4:3 on average – in one case a ratio of 5:1 was observed). Reversed phase silica (Reprosil C18, MeCN, 1 mL/min) proved to be ideal to separate the constitutional isomers **3** and **4** (Figure 3b) in 50 % yield.[25] To identify which peak corresponds to which isomer, 1D and 2D-NMR spectroscopy were performed with the samples obtained from both peaks. ^{1}H-NMR spectroscopy gave a strong indication as to which isomer is which: For the first eluting peak (purple) the signals were again very broad and we quickly suspected it to be the analogous structure of **2**, that is the mismatched helix **4**. The spectra obtained for the second peak (brown) were well defined and sharp at room temperature making it a likely candidate for the uniform analogue **3**. The preliminary assignment was confirmed by 2D-NMR spectroscopy, which allowed explicitly identifying and fully characterizing both *rac*-**3** and *rac*-**4**. As with the sulfur derivative **2**, **4** needed to be heated to 105 °C for deconvolution of the broad signals into an averaged, precise spectrum. The subsequent chiral resolution of *rac*-**3** and *rac*-**4** into the corresponding enantiomers **3a**, **3b**, **4a**, and **4b** under slightly modified conditions (Chiralpak IA, 98:2 hexanes/*i*PrOH, 19 °C) is shown in Figure 3, f-g. The peaks were baseline separated in all cases and the protocol readily up-scaled.

In contrast to the very stable sulfur derivatives **1** and **2**, especially the mismatched selenium oligomer **4** was prone to decompose after several days under oxygen atmosphere at room temperature. Decomposition of the sample was as well observed during the extended periods of measuring variable temperature NMR spectroscopy (VT-NMR) at elevated temperatures – even under oxygen-free conditions. While the quality of the obtained spectra allowed full assignment, the sample could not be recovered after the extensive measurements (approx. 1 week).

Uniform and distorted helices

The previously described structure of diether **5** as elucidated by X-Ray crystallography revealed the expected, ladder like assembly of the six phenyl rings.[23] A highly uniform helix along the terphenylic backbone was found with an overall torsion of 147° and C-O bonds lengths of 1.43 Å. The torsion was determined by measuring the angle between the bottom and top ring of the backbone. One way to explain the high uniformity of the helix is to describe **5** and its new analogues **1** and **3** as a twofold bridged biaryl. The two rings in the middle can be thought of a single biphenyl with all other structural elements being a part of one of the two bridges (top and bottom). Each of the bridges (or better, each ring containing one heteroatom) features 13 atoms, which are similarly arranged (see numbering in Scheme 3) – and hence both rings prefer a similar spatial arrangement. Indeed, the secondary structure of **5** shows a very smooth and continuous helix. In the case of the new model compounds **2** and **4**, the substitution pattern of the relay is reversed and the overall connections of the longer oligomer strand changes from a *meta-ortho-meta-ortho* to a *meta-meta-ortho-ortho* arrangement (see Figure 2, *purple*). From a similar viewpoint as before the rings are no longer containing an equal amount of atoms (bottom: 14, top: 12, see boxes in Scheme 3) nor do they show the same arrangement. Hence each of the rings will prefer a very different spatial arrangement which is expected to translate directly into a distortion of the helix.

While NMR spectroscopy gave indications about some aspects of the adopted structures of **1**-**4** and their relationship to the oxygen analogue, it was fundamentally important to obtain crystals for the sulfur and selenium analogues. Since we expected the halftimes of the enantiopure samples to be in a similar range as for **5** (approximately 9 hours[23]) the racemic mixtures were directly subjected to crystallization. To our great delight suitable conditions for two of the four structures (**1** and **4**) were found after extensive screening of solvent mixtures and crystallization conditions. Both crystallized from hexanes by slow evaporation of the solvent. With all other crystallization attempts we observed exclusive formation of

amorphous material. The recorded diffraction data were excellent for **1** and the obtained structure for the enantiomer **1a** is shown in Figure 4 (*left*). Eventually single crystals suitable for solid state analysis of one of the distorted, more delicate structures (**4**) were obtained. The extremely small, adhered needles made the diffraction analysis demanding but data of suitable quality to determine the solid state structure could be recorded with one of the crystals.

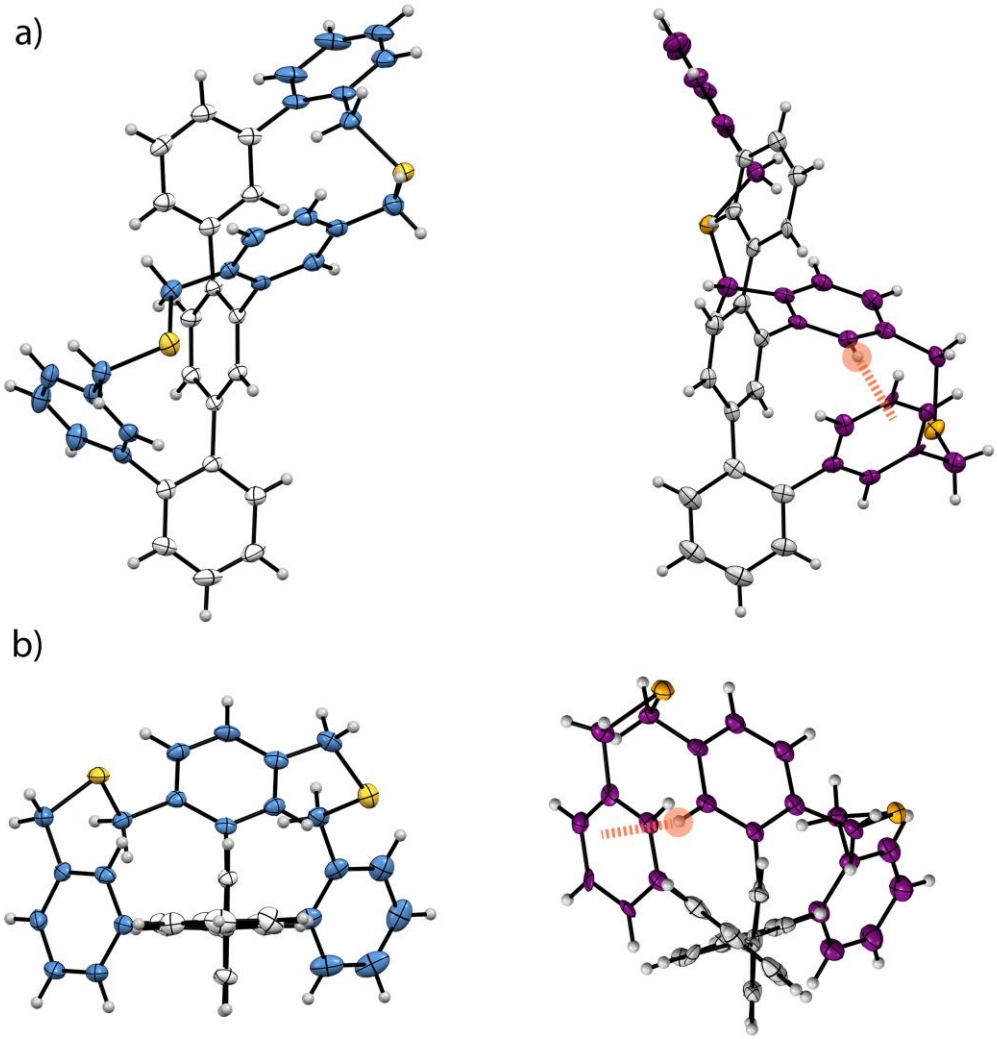

Figure 4: Obtained racemic X-ray structures for **1** and **4** from slow evaporation from hexanes. a) Side-view and b) front-view of **1a** and **4a**. Color code: bridge/blue or purple, backbone/gray, hydrogen atoms/white, sulfur atoms/yellow, selenium atoms/orange. The red circle and dashed line highlight the aromatic proton pointing into the neighboring aromatic ring.

The unit cells are racemic for both **1** and **4** with the enantiomers being present in a 2:2 ratio (see SI S11). The structures were found to be well ordered with a continuous twist of the longer oligomer around the shorter backbone. Only *M* and *P* enantiomers were observed with the twist being relayed from one end of the molecule to the other. The unit cell of **4** revealed a very plausible reason for the challenges we faced when growing and measuring crystals. While the crystallization occurred in pure hexanes, residual trace amounts of ethyl acetate (4 molecules per unit cell) from the previous workup were found in the cell. This finding not only clarifies challenges we faced during attempts to reproduce their crystallization, it also explains why the crystals are so small and fragile: The solvent molecules are arranged within the cells such that they form pores throughout the crystal. These pores presumably facilitate migration and their motion is expected to trigger degradation of the crystal upon temperature alterations.

For the sulfur derivative **1** (Figure 4, *right*), the direct analogue of **5**, considerably increased bond lengths (C-S) were found compared to **5** (1.82 Å vs 1.43 Å). As expected, the targeted increase of the bond lengths had exclusively an impact on the degree of twist (from 147 to 178° when compared to **5**) while maintaining all other aspects of the initial structure like linearity of the backbone and continuity of the helix. In contrast, the selenium containing oligomer **4** shows increased C-Het bond lengths of 1.98 Å in average (1.43 and 1.82 Å for **5** and **1**, respectively) in accordance with the non linear change in size of the heteronuclei. The change of the substitution pattern in the midsection of the wrapping selenoether caused significant changes in the secondary structure. The helix was still found to be continuous with the helicity being transmitted from end to end. However, not only decreased the overall torsion to 121.3 ° (more than 20° less than for **5**), the top and bottom rings of the backbone now deviate about 10° of the relaxed molecular axis. This bending of the backbone is most likely related to the change in ring size (12 and 14 atoms instead of 13 each) and reflects the importance of the original design concept to obtain a stable, continuous helix. A closer look at the individual atoms revealed a rationalization for the high shift of one of the aromatic hydrogens. Only that particular hydrogen points directly into an aromatic ring with a distance of approximately 2.6 Å (Figure 4, highlighted in red). As already discussed during the interpretation of the NMR spectra above, it is therefore strongly affected by the ring current of the neighboring aromatic ring resulting in a strong up-field shift to 5.61 ppm.

It is important to note that despite considerable efforts, we were so far not able to grow suitable crystals from mixtures of *rac*-**2** or *rac*-**3**. Possible reasons include that the structures are subjected to fast conformational changes with related chirality and the apparent strong dependence of crystal growth factors like trace amounts of co-solvents.

CD spectra and racemization barriers of 1-4

Chiral HPLC allowed the separation of the formed isomers of *rac*-**1**-**4** (four for sulfur, and four for selenium, consisting of two constitutional isomers each consisting of a pair of enantiomers). In other words, for each oligomer the corresponding *M* and *P* helices were isolated in high enantiomeric purities (>95 % *ee*). As enantiomers show complementary electronic circular dichroism (ECD) spectra,[27] we recorded ECD and UV/Vis spectra for each isomer, **1a**, **1b**, **2a**, **2b**, **3a**, **3b**, **4a** and **4b** (Figure 5) in 99:1 hexanes/*i*PrOH (for **1** and **2**) and 98:2 hexanes/*i*PrOH (**3** and **4**) immediately after separation by chiral HPLC under air saturated conditions at 10 °C. The reduction of temperature was important to prevent racemization over the timescale of the measurements. Indeed complementary Cotton effects were observed in each case (**1a**,**b**: 244, 224, and 205 nm; **2a,b**: 278, 270, 232, 206 nm; **3a,b**: 288, 254, 232, 206 nm; **4a,b**: 280, 241, 225, 206 nm). The recording of the corresponding UV/Vis allowed to determine the concentrations of the samples in order to normalize the spectra. ECD spectroscopy is routinely used to determine structural similarities between systems. While it is very challenging to deduce a specific arrangement in space based on ECD alone, it is often the case that structural similarities lead to characteristic bands. Once the arrangement is known, it is possible to identify the same arrangement in another, remotely similar system as represented by the importance of ECD spectroscopy in protein characterization and dynamics.[28] High similarities between the spectra of the uniform and the distorted helices were found. For example, **2** and **4** each show a strong band at approx. 280 nm. The same band is, while still present, diminished in the case of **1** and **3**. Similar observations were made for most other bands, pointing at very similar secondary structures of **1** and **3** (and consequently also **2** and **4**). It is therefore likely that the arrangement in space that we have deduced for **1** and **4** by X-Ray diffraction analysis can be transferred to **3** and **2**.

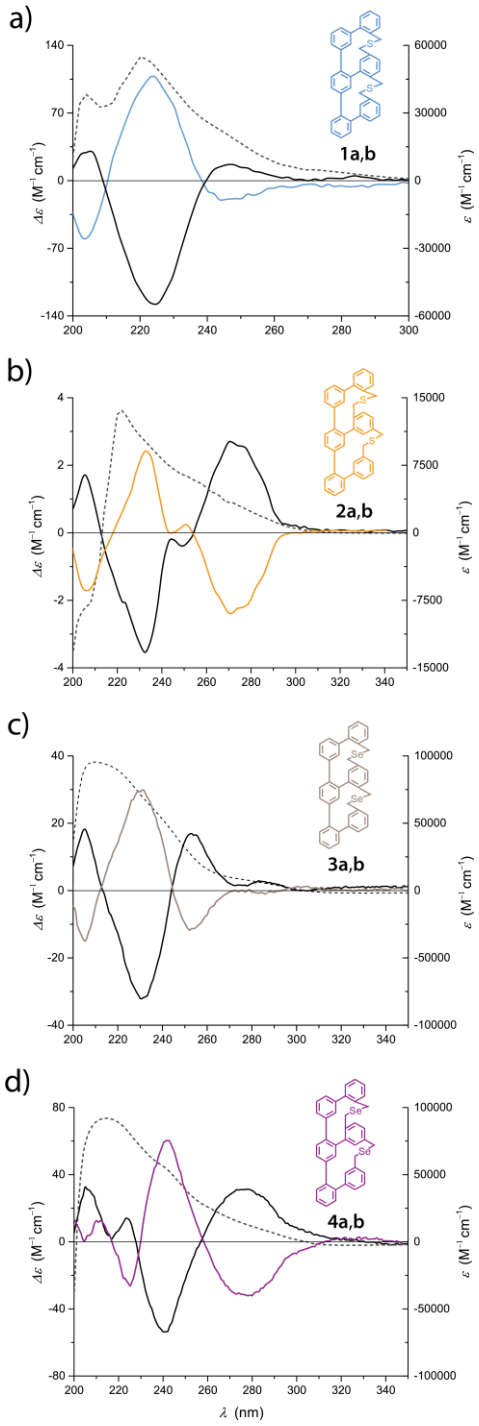

Figure 5*:* UV/Vis (dashed) and CD plots (full) for the sulfur oligomers (a) **1a,b** (b) **2a,b** in 99:1 hexanes/*i*PrOH at 10 °C and the selenium oligomers (c) **3a,b** and (d) **4a,b** in 98:2 hexanes/iPrOH at 10 and 5 °C, respectively.

Both samples **1** and **4** crystallized with racemic unit cells and thus the solid state analysis did not allow to determine the absolute configuration. The arrangement of the chromophores in space can in some cases be determined directly from the obtained ECD spectra but this requires well resolved exciton coupling bands, which was not the case for any of the systems presented here. However, the strong, distinct *Cotton* bands in the ECD spectra offered an opportunity to determine the absolute conformation *in silico*, especially as we could profit from the single crystal structures as starting points for the calculations. Also the mainly carbon based scaffold of the structures simplified the calculations significantly. To take the softer heteroatoms into account, calculations were performed with the B3LYP/6-31G** basis set, which already demonstrated its accuracy for systems involving heteroatoms.[29] Structure optimizations and subsequent time dependent calculations (TD-B3LYP/6-31G**, 150 states) with 75 triplet und 75 singlet excitations were performed and the obtained signs of the Cotton bands compared with the experimental spectra (Figure 6). In spite of the rather rudimentary approach, good enough agreement between predicted and recorded ECD spectra were observed in all cases, enabling the assignment of **1a** - **4a** and **1b** - **4b** to the *P* and *M* helices, respectively.

Based on this assignment of the absolute configurations the recorded HPLC traces were re-evaluated. For the uniform cases (**1** and **3**), the *P* helices are eluting before their enantiomeric counterpart, while in the case of the distorted helices **2** and **4** the order is reversed. We thus conclude that the secondary structure of the constitutional isomers is considerably different such that the interaction with the chiral stationary phase leads to inversion of the elution order.

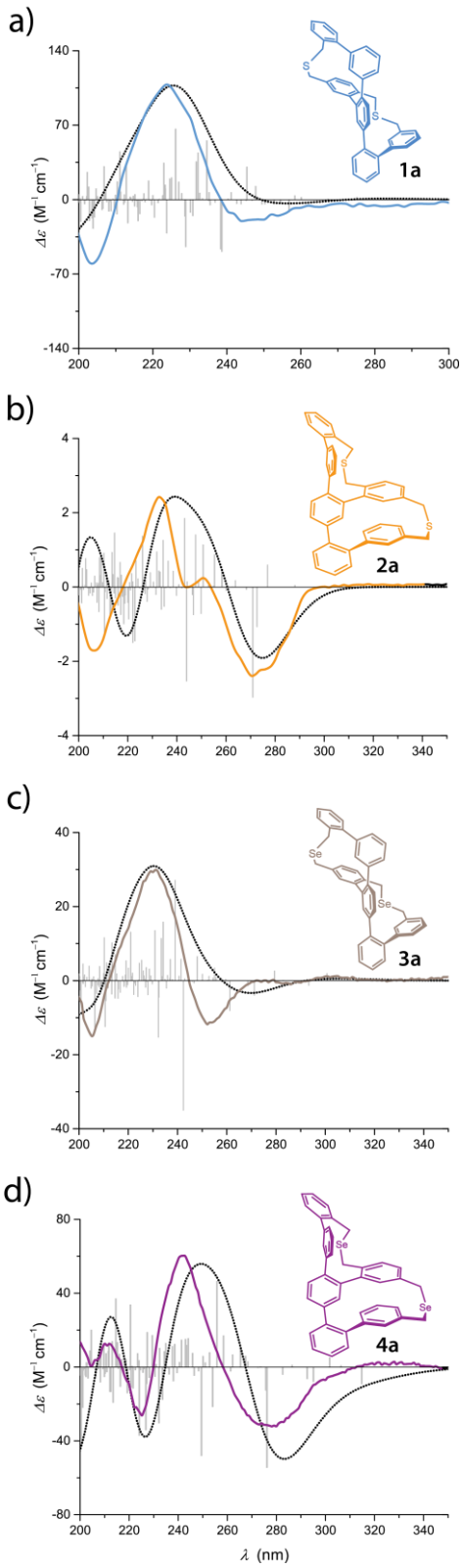

Figure 6: Experimental and calculated ECD spectra of **1a** - **4a** using TD-B3LYP/6-31G** with 75 triplet und 75 singlet excitations; total: 150 states; width 0.4 eV. The calculated spectra are based on the conformer with minimal energy. Colored: experimental spectra; black: calculated spectra, bars: calculated transitions.

Dynamics of the helices 1-4

ECD spectroscopy not only allows the investigation of chiral phenomena as such but also enables the observation of racemization and enantiomerization processes.[30-33] We were interested to compare the racemization barriers with the already known ether analogue **5**. Of particular interest was the impact of the elongated bridges (**1** and **3**) and the mismatched ring sizes in **2** and **4** on the racemization process. A racemic sample of each derivative **1** - **4** (~0.2 mg/mL) in the eluent was prepared. 300 µL of that solution were injected and the enantiomers separated by chiral HPLC (Chiralpak IA, 4 mL/min, 99:1 hexanes/*i*PrOH, 18 °C for **1** and **2**, 1 mL/min, 98:2 hexanes/*i*PrOH, 19 °C for **3** and **4**). A sample of the *P* conformer (**1a** – **4a**) was collected after chiral HPLC and immediately subjected to ECD spectroscopy. Over a set amount of time, 50 points were recorded at the most intense Cotton band (**1a**: 222 nm; **2a**: 230 nm, **3a**: 230, **4a**: 241 nm) at 25 °C until complete disappearance of the CD signal displayed that the racemate was reached.[34]

Figure 7 shows the exponential decay for both **1a** and **2a**. As the racemization process is not mediated by another molecule, the kinetics are expected to be of 1st order. If valid, linearization of the data by plotting time vs ln(A) gives direct access to the rate constant of racemization k_{rac} and eventually to the racemization barrier $\Delta G^{\ddagger}_{rac}$ at 25 °C. The data was found to be linear (and hence 1st order) resulting in excellent fits in all cases. The obtained values are summarized in **Table 1**.

		link	C-Het [Å]	Torsion [°]	$\Delta \boldsymbol{G}^{\ddagger}_{\boldsymbol{rac}}$ [kJ mol^{-1}]
uniform	**5**	O	1.43	147	97.6 ± 0.1
	1a	S	1.82	178	97.2 ± 0.1
	3a	Se	1.98[a]	146	90.4 ± 0.1
distorted	**2a**	S	1.86[a]	126	96.0 ± 0.1
	4a	Se	1.98	121	96.2 ± 0.1

Table 1: The measured racemization barriers at 25 °C for **1a** - **4a** from the corresponding linear fits including the value for the diether **5** (*P* helices). The corresponding bond lengths and torsions of the backbone are given for comparison. [a]Computed values

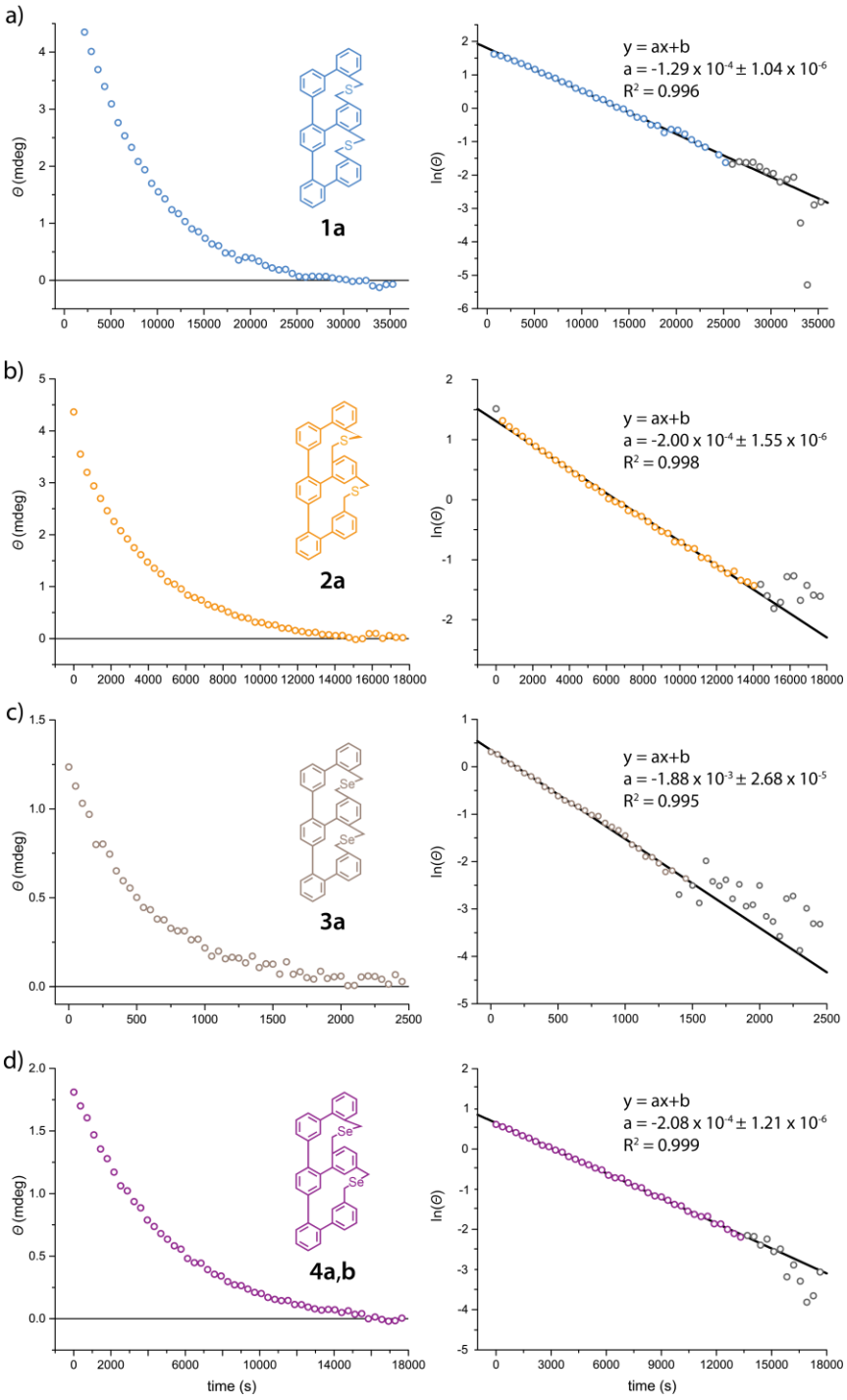

Figure 7: Decay of the CD signals for the oligomers **1**-**4**. After isolation of one corresponding enantiomer the loss of CD signal was observed at ΔA_{max} at 25 °C over time. Linear fitting of ln(A) vs time allowed to access the rate constant of racemization k_{rac} and with that the racemization barrier $\Delta G^{\ddagger}_{rac}$ at 25 °C.

Particularly interesting was to see changes in the values of $\Delta G^{\ddagger}_{rac}$ for the well ordered helices **1** and **3**. The thioether **1** gives a racemization barrier which is very similar to the (oxygen)ether bridged oligomer **5** ($\Delta\Delta G^{\ddagger}_{rac}$ = 0.4 kJ mol^{-1}). Apparently, the length of the bond (1.43 vs 1.82 Å for **5** and **1**, respectively) which translates directly into an increased twist (147° vs 178°) as obtained by X-Ray diffraction analysis has almost no impact on the rate of racemization. We thus rationalize that the larger and softer sulfur atoms allow the adaption of a greater variety of angles, compensating for the increased twist. As for **5** the transition from the *M* to the *P* conformer (and vice versa) is smooth without any observable intermediate on the timescale of the experiments. The selenium analogue **3** is the key structure to deduce which of the opposing trends will dominate. Exchanging oxygen for sulfur and selenium means a continuous increase in the atomic radius and further elongated bonds (and thus presumably an even higher overall torsion). On the other hand, the larger and softer atom results in an even less defined angle at the heteroatom, which is expected to further reduce the racemization barrier. If a further increased value of $\Delta G^{\ddagger}_{rac}$ is found, the increased torsion helps to stabilize the helix while a reduced racemization barrier might indicate that the softer nucleus allows the interconversion to proceed more readily. As for both **5** and **1**, the observed racemization is well behaved and undergoes a direct interconversion. Strikingly, the obtained barrier is significantly decreased ($\Delta\Delta G^{\ddagger}_{rac}$ about 7 kJ mol^{-1}) clearly deviating from the other two model compounds. As it was not possible to obtain a crystal structure for the selenium derivative **3** we relied on the B3LYP optimized *in silico* geometry (Figure 8) that we used to calculate the CD spectra. We based the structure on the solid state structure of **1** and exchanged sulfur for selenium. The obtained structure revealed significantly reduced torsion angles compared to **1** (146° instead of 178°). However, the found average C-Se bond length (1.98 Å) was identical to that of the distorted selenodiether **4**. As the calculated CD spectra is in very good agreement to the experimental data we have strong reason to assume the calculated structure to be accurate. We surmise that the further elongation of the C-Het bond does no longer increase the overall torsion. Contrary to the sulfur helix **3**, where the elongation leads to an increase of torsion and that in turn compensates the enhanced flexibility of the heteroatom, these trends are no longer counteracting and very likely the reason for the significantly reduced racemization barrier.

We next turned our attention to the two mismatched helices. As outlined before, both **2** and **4** show broad NMR signals for the protons of the bridge which indicates the presence of multiple, rapidly interchanging conformers. However, we do not consider them to be racemization processes but rather fast, small conformation changes of the bridge as the protons on the backbone are well defined and sharp. That the racemization processes are generally much slower than the NMR timescale is clearly supported by the

successful separation of the enantiomers by chiral HPLC. Again, the clear doublet in the HPLC trace and the resulting complementary CD spectra strongly suggest that only two types of long-lived helices are present. Furthermore, heating the samples resulted in averaged, well defined spectra, indicating that the barrier for these small conformation changes is low. It is thus not surprising that the observed CD decays and the subsequent plot of ln(A) vs time showed excellent linear behavior and very well defined values of $\Delta G^{\ddagger}_{rac}$ (96.0 ± 0.1 mol^{-1} for **2** and 96.2 ± 0.1 kJ mol^{-1} for **4**). Neither the uniformity of the helix nor the enlarged ring size has a significant impact on the racemization barrier the measured values are only marginally lower than that of the uniform helices ($\Delta\Delta G^{\ddagger}_{rac}$ ~1 kJ mol^{-1}). Furthermore, the mismatched helices do not follow the trend set by the matched derivatives upon exchanging of the heteroatom. The torsion angle (**2**, calculated: 126°; **4**, measured: 121°) changes only marginally while the barrier increased by $\Delta\Delta G^{\ddagger}_{rac}$ = 0.1 kJ mol^{-1} which is smaller than the accuracy of the method. Based on these findings we conclude that either the racemization process of these distorted oligomers does not rely on the size or nature of the incorporated heteroatom, or there are two competing features at work which compensate each other perfectly in the two model compounds. In similarity to the model compounds **1**, **3** and **5**, we currently favor the second hypothesis.

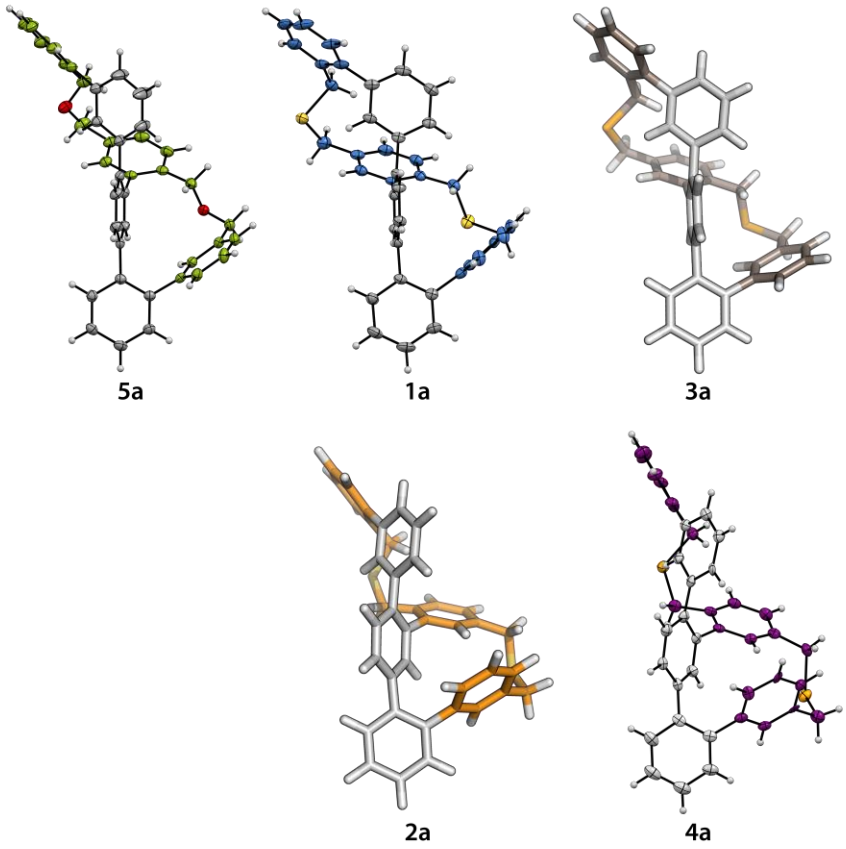

Figure 8: Solid states structures by X-ray diffraction analysis(**5a**, **1a**, **4a**) and calculated structures (**2a** and **3a**) using Gaussian and B3LYP/6-31G**. The top row depicts the matched helices with a smooth helical wrapping of the longer oligomer. The lower row shows the mismatched, distorted helices. In all cases continuous wrapping of the longer oligomer was determined (or predicted) giving only one pair of enantiomers (*M* and *P*) each.

Conclusion

In this work new types of chiral ladder systems that show induced, elongated or distorted helicity are assembled via an efficient synthetic route. The studies demonstrate conceptually and experimentally that elongation of the bridge alters mainly the degree of twist while changes in ring size leads to distortion of the helix. More accurately, the modulation of the overall torsion with the alteration of the heteroatoms and the distortion of the helices by a targeted change in the substitution pattern of the relay are demonstrated. Accessing of the new derivatives was possible due to a short synthetic route, which includes minimal amounts of borylations, precise regioselective halogenation mediated by a neighboring boronic ester and *Appel*-type substitution of two benzylic hydroxy groups to a versatile, modular precursor. This precursor allowed for two consecutive macrocyclizations and the successful integration of either two sulfur or selenium atoms in a single synthetic step. The flexibility of the precursor gave access

to two further (constitutional) isomers with an inverted substitution pattern on the relay. The total of eight structures - for each type of heteroatom two structural isomers which exist as enantiomeric pairs – were accessed in high yields and separated into the individual isomers by a multitude of chromatographic protocols (both achiral and chiral). Extensive NMR spectroscopy and High Resolution-MS allowed to unambiguously identify each structure while ECD spectroscopy of the purified isomers allowed to confirm similar secondary structures and identify the enantiomeric pairs. *In silico* ECD-calculations allowed to assign the absolute stereochemistry of the enantiomers and project the arrangement of the helices in space. The structural arrangements of two of the four structural isomers was confirmed by X-Ray diffraction analysis revealing alteration of the secondary structure upon changing of the substitution pattern (uniform and distorted helix). Elongation of the heteroatomic bonds increased the torsion angle in the case of the sulfur system while decreased torsion was observed for the selenoether. Two dynamic processed were investigated: VT-NMR spectroscopy for the distorted helices and the racemization processes of all four model compounds by ECD decay spectroscopy. VT-NMR demonstrated that the bridge of the distorted helix derivatives is flexible and can undergo small structural changes on the NMR timescale as indicated by the broad signals at 25 °C that coalesce at elevated temperatures. The protons of the backbone are sharp at room temperature which is consistent with a racemization process on a larger timeframe. The observation of decay of the most prominent *Cotton* band by ECD lead to precise values for the racemization barrier and allowed to relate the racemization to the spatial arrangement of the structures. Two main trends were found: The length of the heteroatomic bonds (increased torsion) and the size of the heteronucleus (softer nuclei with less defined bond angles) are compensating each other in the case of sulfur. The much larger selenium shows a highly reduced racemization barrier in the case of the uniform helix due to a reduced torsion angle *and* a softer nucleus. In both cases the distorted helices do not respond to the change in heteroatom. The prevention of an achiral *meso* form, the continuity of the induced helices and the observed uniform racemization pathways made the study of these fascinating structures possible.

The prospect of introducing a variety of linkages is an important step towards stable “Geländer” type helices. As the ring size was found to play a crucial role in the stereodynamics and spatial arrangement of the oligomer, a more constrained helix with decreased ring sizes becomes desirable. Especially sulfur is an ideal entry point to access all carbon based, tighter derivatives. A further option towards long term stable helices is the elongation of the helix leading to longer ladders with increased overall torsions. These studies are currently ongoing and will be reported in due course.

References

[1] J. L. Alonso-Gómez, P. Rivera-Fuentes, N. Harada, N. Berova, F. Diederich, *Angew. Chem. Int. Ed.* **2009**, *48*, 5545–5548.

[2] W. Nakanishi, T. Matsuno, J. Ichikawa, H. Isobe, *Angew. Chem. Int. Ed.* **2011**, *50*, 6048–6051.

[3] K. S. Hayes, M. Nagumo, J. F. Blount, K. Mislow, *J. Am. Chem. Soc.* **1980**, *102*, 2773–2776.

[4] G. S. Kottas, L. I. Clarke, D. Horinek, J. Michl, *Chem. Rev.* **2005**, *105*, 1281–1376.

[5] Y. Wang, A. D. Stretton, M. C. McConnell, P. A. Wood, S. Parsons, J. B. Henry, A. R. Mount, T. H. Galow, *J. Am. Chem. Soc.* **2007**, *129*, 13193–13200.

[6] H. Ito, T. Abe, K. Saigo, *Angew. Chem. Int. Ed.* **2011**, *50*, 7144–7147.

[7] S. Nobusue, Y. Mukai, Y. Fukumoto, R. Umeda, K. Tahara, M. Sonoda, Y. Tobe, *Chem. Eur. J.* **2012**, *18*, 12814–12824.

[8] R. A. Pascal, *Chem. Rev.* **2006**, *106*, 4809–4819.

[9] C. S. Hartley, *J. Org. Chem.* **2011**, *76*, 9188–9191.

[10] T. Kudernac, N. Ruangsupapichat, M. Parschau, B. Maciá, N. Katsonis, S. R. Harutyunyan, K-H. Ernst, B. L. Feringa, *Nature* **2011**, *479*, 208-211.

[11] M. Gingras, *Chem. Soc. Rev.* **2013**, *42*, 968–1006.

[12] M. Gingras, G. Félix, R. Peresutti, *Chem. Soc. Rev.* **2013**, *42*, 1007–1050.

[13] M. Gingras, *Chem. Soc. Rev.* **2013**, *42*, 1051–1095.

[14] B. Kiupel, C. Niederalt, M. Nieger, S. Grimme, F. Vögtle, *Angew. Chem. Int. Ed.* **1998**, *37*, 3031–3034.

[15] M. Modjewski, S. V. Lindeman, R. Rathore, *Org. Lett.* **2009**, *11*, 4656–4659.

[16] K. Ohkata, R. L. Paquette, L. A. Paquette, *J. Am. Chem. Soc.* **1979**, *101*, 6687–6693.

[17] K. Müllen, W. Heinz, F.-G. Klärner, W. R. Roth, I. Kindermann, O. Adamczak, M. Wette, J. Lex, *Chem. Ber.* **1990**, *123*, 2349–2371.

[18] L. Venkataraman, J. E. Klare, C. Nuckolls, M. S. Hybertsen, M. L. Steigerwald, *Nature* **2006**, *442*, 904–907.

[19] D. Vonlanthen, A. Mishchenko, M. Elbing, M. Neuburger, T. Wandlowski, M. Mayor, *Angew. Chem. Int. Ed.* **2009**, *48*, 8886–8890.

[20] J. Rotzler, H. Gsellinger, A. Bihlmeier, M. Gantenbein, D. Vonlanthen, D. Häussinger, W. Klopper, M. Mayor, *Org. Biomol. Chem.* **2012**, *11*, 110–118.

[21] D. P. Iwaniuk, K. W. Bentley, C. Wolf, *Chirality* **2012**, *24*, 584–589.

[22] S. Menning, M. Krämer, B. A. Coombs, F. Rominger, A. Beeby, A. Dreuw, U. H. F. Bunz, *J. Am. Chem. Soc.* **2013**, *135*, 2160–2163.

[23] M. Rickhaus, L. M. Bannwart, M. Neuburger, H. Gsellinger, K. Zimmermann, D. Häussinger, M. Mayor, *Angew. Chem. Int. Ed.* **2014**, *53*, 14587–14591.

[24] M. Rickhaus, L. M. Bannwart, O. Unke, H. Gsellinger, D. Häussinger, M. Mayor, *Eur. J. Org. Chem.* **2015**, *2015*, 786–801.

[25] About 25 % of the remaining yield was attributed to structures containing three selenium atoms, most likely to systems containing each one selenium and one diselenium bridge as indicated by HR-ESI-MS.

[25] F. Mo, J. M. Yan, D. Qiu, F. Li, Y. Zhang, J. Wang, *Angew. Chem. Int. Ed.* **2010**, *49*, 2028–2032.

[26] D. Qiu, F. Mo, Z. Zheng, Y. Zhang, J. Wang, *Org. Lett.* **2010**, *12*, 5474–5477.

[27] For an excellent tutorial, see: N. Berova, L. D. Bari, G. Pescitelli, *Chem. Soc. Rev.* **2007**, *36*, 914–931.

[28] For a comprehensive introduction, see: G. Pescitelli, L. D. Bari, N. Berova, *Chem. Soc. Rev.* **2011**, *40*, 4603–4625.

[29] G. S. Heverly-Coulson, R. J. Boyd, *J. Phys. Chem. A* **2011**, *115*, 4827–4831.

[30] P. Osswald, F. Würthner, *J. Am. Chem. Soc.* **2007**, *129*, 14319–14326.

[31] H. Saito, T. Mori, Y. Origane, T. Wada, Y. Inoue, *Chirality* **2008**, *20*, 278–281.

[32] L. Lunazzi, M. Mancinelli, A. Mazzanti, M. Pierini, *J. Org. Chem.* **2010**, *75*, 5927–5933.

[33] S. Ando, E. Ohta, A. Kosaka, D. Hashizume, H. Koshino, T. Fukushima, T. Aida, *J. Am. Chem. Soc.* **2012**, *134*, 11084–11087.

[34] Measuring **3a** in 99:1 hexanes/*i*PrOH gave an identical spectrum. For convenience and reproducibility, the respective eluent of the HPLC run was chosen for the CD measurements.

Keywords

Atropisomerism, helical structures, racemization, conformation analysis, ladder oligomer

Graphical Abstract

Evolution of a twisted ladder: A ladder oligomer adopts a helical conformation due to the size mismatch of the rails. Upon elongation of the chain-length between neighboring rings, the system responds by an increased twist. Changing the substitution pattern of the relay results in the distortion of the helix.